Available online at www.sciencedirect.com
SCIENCE DIRECT®
ELSEVIER
International Journal of Mass Spectrometry 228 (2003) 1017–1034
International Journal of Mass Spectrometry
www.elsevier.com/locate/ijms

Hydration of cyclic oxocarbon dianions, such as c-$C_5O_5^{2-}$, in the gas phase. Charge reduction of hydrates by electron detachment or proton transfer Energy barriers for electron detachment and electron transfer

T. Blades Arthur, Michael Peschke, Paul Kebarle*

Department of Chemistry, University of Alberta, Edmonton, Alta., Canada, T6G 2G2

Received 21 January 2003; accepted 25 April 2003

Dedicated to Prof. Helmut Schwarz on the occasion of his 60th birthday

Abstract

The cyclic oxocarbon dianions $C_nO_n^{2-}$ are known to exist in aqueous solution, but have not been previously produced in the gas phase. Using electrospray, the $n = 5$ (croconate) and $n = 6$ (rodhizonate) dianions were easily observed in the gas phase. Croconate was used for all further studies. The dianion was observed only when solvated by two or more H_2O molecules. The hydration equilibria $(n-1,n)$ for the croconate dianion: $C_5O_5(H_2O)_{n-1}^{2-} + H_2O = C_5O_5(H_2O)_n^{2-}$ were determined for $n = 3$–9, with a reaction chamber attached to a triple quadrupole mass spectrometer, obtaining thus values for ΔG°, ΔH° and ΔS° of the above hydration reactions. At temperatures above 50 °C and low water partial pressures that led to hydrates below $n = 2$, charge reduction by electron detachment was observed. Solvents with higher gas phase acidity, such as methanol, led to charge reduction by proton transfer from methanol to the dianion. The $C_5O_5(H_2O)_2^{2-}$ was stable towards electron detachment even though the electron affinity of the monoanion $EA(C_5O_5(H_2O)_2^-)$ evaluated at the B3LYP/6-311++G(d,p) level was negative. This result demonstrates that the electron detachment is impeded by the existence of a Coulomb barrier for the reverse, electron attachment, reaction. Electron transfer from the dianions to neutral molecules B that have positive electron affinities, such as nitrobenzene, is also impeded by a Coulomb barrier. This is indicated by the formation of complexes $(C_5O_5(H_2O)_nB_m)^{2-}$ at 50 °C and lower temperatures, in which the double charge has remained on the C_5O_5 group. The bonding in $(C_5O_5(H_2O)_nB_m)^{2-}$ is discussed. However, electron transfer to compound B with higher electron affinities such as di-nitrobenzene is observed at 50 °C.

Keywords: Oxocarbon dianions; Electron detachment; Hydration

1. Introduction

1.1. Oxocarbon dianions history

The cyclic oxocarbon dianions $C_nO_n^{2-}$: deltate **1**, squarate **2**, croconate **3** and rodhizonate **4**

* Corresponding author. Tel.: +1-780-492-3469; fax: +1-780-492-8231.
E-mail address: paul.kebarle@ualberat.ca (P. Kebarle).

1387-3806/$ – see front matter © 2003 Elsevier B.V. All rights reserved.
doi:10.1016/S1387-3806(03)00267-7

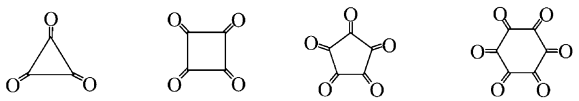

1 2 3 4

were probably the first organic compounds produced by synthesis. Gmelin in an attempt to obtain metallic potassium by the reduction of potassium hydroxide with carbon in 1825, obtained instead dipotassium croconate from the black powdery residue. This synthesis predates the classical synthesis of urea by Wohler in 1828 [1]. The salts in the solid state as well as the dianions that form in aqueous solution are quite stable. The electronic stabilization of the dianions has also been examined [2].

These symmetric cyclic dianions are of interest to gas phase ion chemistry involving multiply charged ions. The field of multiply charged ion chemistry has expanded rapidly [3–6] since the advent of electrospray ionization (ESI) [7]. The Refs. [3–6] include only the earliest and some of the most recent work. In the gas phase, the multiply charged ions are strongly affected by the Coulombic repulsion between the charges. This repulsion often can lead to charge reduction by dissociation to two charged products (charge separation). This process is fostered by the proximity of the charge in the original multiply charged ion and for doubly charged systems two classes have been studied.

1.2. Multiply charged metal ions

The double charge is on one relatively small unit such as in $Ca(H_2O)_2{}^{2+}$. The addition of the first H_2O molecule to the Ca^{2+} ion leads to straightforward hydration. However, when the second molecule is supplied, the dihydrate undergoes charge separation:

$$Ca(H_2O)_2{}^{2+} = CaOH^+ + H_3O^+ \quad (1)$$

in the absence of very rapid collisional stabilization by third body gas collisions [8]. In experiments where one starts with the higher hydrates $Ca(H_2O)_n{}^{2+}$, as would be the case for ions produced by ESI from aqueous solution [4], gradual desolvation at higher temperature or via collision-induced dissociation (CID), that initially leads to simple H_2O loss, is replaced by charge separation at $n = 2$, i.e., reaction (1). In both of these cases, the charge separation is a consequence of the dissociation kinetics as shown below.

Several theoretical computations of the energy change and transition state of charge separation reactions like Eq. (1) are available [9–13]. Concerning reaction (1) these show that the energy released on formation of $Ca(H_2O)_2{}^{2+}$ from Ca^{2+} and H_2O is considerably higher than the energy of the transition state for charge separation so that charge separation dominates over back dissociation, in the absence of rapid collisional quenching [11]. Of special interest are also the findings that the transition state involves a salt bridge structure in which M retains an approximate double charge character, the hydroxy O atom, a negative charge and the H of the H_3O^+ a positive charge [11–13]. Photodissociation results in which a large kinetic energy release was determined, as expected for these Coulombic repulsion driven reactions, has been reported for the charge separation of the $Co(H_2O)_4{}^{2+}$ ion [14].

1.3. Two or more singly charged groups on the same molecule

The diprotonated alkyl diamines such as $(NH_3(CH_2)_nNH_3)^{2+}$ are typical examples of systems with two charged groups. The stability of these systems increases as the length of the alkyl chain is increased. It increases also with solvation by H_2O [15]. However, the presence of solvent molecules can also lead to loss of charge due to charge separation as was the case for multiply charged metal ions. Experimental studies of $(NH_3(CH_2)_nNH_3{\cdot}B)^{2+}$, where $B = NH_3$, $MeNH_2$ and other weaker and stronger gas phase bases have been made [16] to examine the conditions under which charge separation occurs. For these systems when B leads to charge separation, the gas phase basicity of B is equal or higher than the apparent gas phase basicity GB^{app} of the deprotonated group of the diamine [16–19]. GB^{app} depends

not only on the intrinsic basicity of the group that holds the proton but also on the Coulombic repulsion due to the other charge(s) that is (are) present. Relationships for GB^{app} and the distance between the charged groups can be obtained from comparison of experiment with theory [16–19]. The resulting equations can be applied also to multiply protonated proteins produced by electrospray [16]. This approach can be used to obtain important insights concerning the origin of the observed charge states of proteins [16,20].

Dianions, from deprotonated carboxylic acids, such as $(CO_2(CH_2)_nCO_2)^{2-}$ and their solvation or charge loss induced by proton transfer from the solvent molecule, provide similar information for the negative ion states, that also can be applied to charge states of proteins observed in the negative ion mode [20b].

Charge loss involving multiply charged negative ions can occur also by electron loss. This may be direct electron loss by thermal electron detachment [21] or due to electron transfer to the solvent molecule, when these molecules have a positive electron affinity, which is not common. Charge loss by electron loss is unique to negative ions in the gas phase. Anions of great importance in the condensed phase such as SO_4^{2-} and PO_4^{3-} are unstable in the gas phase due to electron loss. Thus, naked SO_4^{2-} cannot be observed. At least two to three water molecules are required to achieve stabilization [22].

1.4. Oxocarbon dianions in the gas phase

The cyclic oxocarbon dianions such as **3** and **4** obviously fall in a special class, because the charge is symmetrically distributed over a cyclic system. Thus, their gas phase ion chemistry is worthy of study (vide infra), even though these systems cannot be expected to lead to as many applications as the other multiply charged ions discussed above. The dianions **3** and **4** are readily obtained in the gas phase by ESI from methanol or methanol–water solutions of the sodium salts. To our knowledge, this is the first production and study of these ions in the gas phase.

2. Experimental conditions and theoretical calculations

2.1. Experimental

The experiments were performed with an apparatus that includes a reaction-equilibration chamber whose temperature can be controlled [15]. A sampling capillary, located about 1 cm away from the electrospray tip, leads to a fore chamber and a reaction chamber. Use of a counterflow of curtain gas N_2 at the entrance of the sampling capillary prevents solvent vapor from entering the fore chamber. The fore- and reaction-chambers are maintained at 10 Torr N_2 (bath gas) pressure by a separate capillary that enters the reaction chamber and carries N_2 and known partial pressures of reagent gases in the mTorr range. An electric field drifts the ions from the fore- to the reaction-chamber. A weak electric field drifts the ions in the reaction chamber to an exit leak where the escaping gas and ions enter the vacuum containing a QqQ mass spectrometer. The drift times of the ions, through the reaction chamber that correspond to the ion reaction times are in the 100–300 μs range depending on the value of the drift field used. For more details about apparatus and conditions, see [15].

The croconate **3** and the rodhizonate **4** ions were obtained from a 10^{-4} M solution of the sodium salts in methanol–water using ESI flow rates of 1 μL/min. The salts were obtained from Aldrich and used without further purification.

Neat water or high water content methanol solutions could not be used because of electric discharges. Even with the methanol water solutions electric discharges had to be suppressed by addition of low concentrations of SF_6 to the air.

2.2. Calculations

All calculations were performed using Gaussian94 [23]. The B3LYP density functional method was chosen because it has yielded reliable hydration energies in the past for various ion–molecule systems with

errors bars of 2–3 kcal/mol [10]. As a basis set, the 6-311++G(d,p) basis set was chosen. The triple zeta basis set plus polarization and diffuse functions is necessary for a reasonable description of the more diffuse orbitals of anions. However, based on tests generally DFT does not benefit significantly from larger basis sets once a reasonable large one such as the one chosen for these calculations is used.

3. Results and discussion

3.1. Solvation stabilizes the cyclo oxocarbon, c-$C_5O_5^{2-}$, dianion. Activation of the weakly solvated hydrate $C_5O_5(H_2O)_2^{2-}$, leads to electron detachment

The mass spectra of the negative ions observed in the presence of water vapor in the reaction chamber at 22 °C are shown in Fig. 1a and b. The $C_5O_5^{2-}$ hydrates, $C_5O_5(H_2O)_n^{2-}$, are the dominant ions. The only extraneous ion with significant intensity is at *m/z* 93 and corresponds to $CH_3OCO_2(H_2O)^-$. This is an ion that we practically always observe whenever methanol is sprayed in the negative ion mode. At the lower H_2O partial pressure of 2 mTorr, the hydrates, $C_5O_5(H_2O)_n^{2-}$ have a maximum intensity for $n = 4$ while at the higher water pressure of 10 mTorr (Fig. 1b), the maximum has shifted to $n = 5$, and hydrates of high intensity up to $n = 6$ and 7 ($m/z = 142$) are also detected. At H_2O pressures in the mTorr range, the hydrates are at equilibrium. Equilibrium constants obtained at different H_2O pressures and different temperatures will be presented in Section 3.3.

The spectra in Fig. 2a and b were obtained at the same two water pressures as in Fig. 1, but at a higher temperature, 52 °C. The $C_5O_5(H_2O)_n^{2-}$ ions are shifted to lower *n*, as expected. At $pH_2O = 2$ mTorr, the lowest hydrate observed is $C_5O_5(H_2O)_2^{2-}$. This is the lowest hydrate that could be observed at temperatures higher than 55 °C and low water partial pressures, which are conditions where the presence of the monohydrate $C_5O_5(H_2O)^{2-}$ would be expected had it been stable.

Furthermore, CID experiments with the QqQ involving $C_5O_5(H_2O)_n^{2-}$ precursor ions with $n = 5$, 4 and 3 led to a lowest visible product, $C_5O_5(H_2O)_2^{2-}$, but not to $C_5O_5(H_2O)^{2-}$. The observed singly charged CID products were $C_5O_5(H_2O)^-$ and $C_5O_5^-$. The product spectrum from CID of $C_5O_5(H_2O)_4^{2-}$ is given in Fig. 3. The results indicate that the monohydrate $C_5O_5(H_2O)^{2-}$ and the bare $C_5O_5^{2-}$ ion are unstable and that loss of charge occurs by thermal electron detachment [21] in the experiments (Fig. 2) and CID activated electron detachment (Fig. 3). The two modes are related since in both cases internal (ro-vibrational) excitation is involved.

$$C_5O_5(H_2O)^{2-} = C_5O_5(H_2O)^- + e^- \quad (2a)$$

$$C_5O_5^{2-} = C_5O_5^- + e^- \quad (2b)$$

In the CID experiments, only the $C_5O_5^-$ and $C_5O_5(H_2O)^-$ products were observed, but in Fig. 2a and b, both $C_5O_5^-$ and $HC_5O_5^-$ are observed. The formation of $HC_5O_5^-$ might have been attributed to proton transfer from one of the H_2O molecules followed by charge separation. However, a more detailed investigation shows that this is not the case. Results at 55 °C, obtained at several different H_2O pressures, are given in Fig. 4. The decrease of the singly charged $C_5O_5^-$, with increase of water pressure, is much more pronounced than is the case for the $HC_5O_5^-$ ion. The absence of change for $HC_5O_5^-$ indicates that this ion is not a product of proton transfer from water.

The $Na_2C_5O_5$ salt was sprayed in a methanol solution, see Section 2.1. Under these conditions, the initial $C_5O_5^{2-}$ ions obtained from the electrospray will be solvated by methanol molecules. Therefore, some protonation of the $C_5O_5^{2-}$ by CH_3OH could be occurring after the $C_5O_5(CH_3OH)_m^{2-}$ ions enter the heated fore chamber of the apparatus (see Section 2.1). Based on the gas phase acidities of H_2O and CH_3OH [25,26], the free energy for protonation by CH_3OH is ~8.7 kcal/mol more favorable relative to protonation by H_2O. The spectrum shown in Fig. 5 was obtained with 5. 5 mTorr of CH_3OH in the reaction chamber at 25 °C. It exhibits high intensities of the singly charged ions $HC_5O_5^-$ and $CH_3O(CH_3OH)_n^-$. These

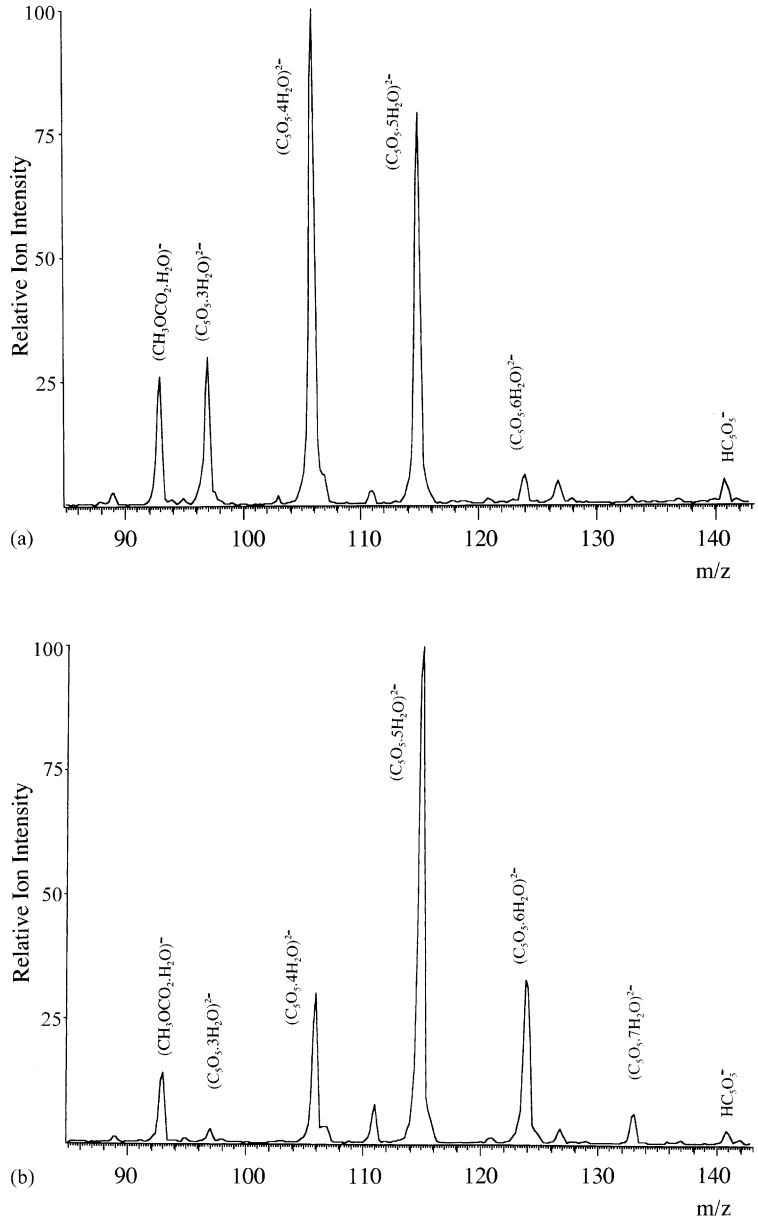

Fig. 1. (a) Mass spectrum of hydrates $C_5O_5(H_2O)_n^{2-}$ observed at 22 °C and 2 mTorr of H_2O vapor in reaction chamber. $C_5O_5(H_2O)_5^{2-}$ is the last hydrate of high intensity. (b) Mass spectrum of hydrates $C_5O_5(H_2O)_n^{2-}$ observed at 22 °C and 10 mTorr of H_2O vapor in reaction chamber. Intense hydrates observed up to $C_5O_5(H_2O)_7^{2-}$ at this higher H_2O pressure.

singly charged ions must be due to proton transfer from CH_3OH, followed by charge separation:

$$C_5O_5(CH_3OH)_m^{2-} = HC_5O_5(CH_3OH)_{m-x}^{-} + CH_3O(CH_3OH)_{x-1}^{-} \quad (3)$$

These results support the assumption based on Fig. 4, that the observed $HC_5O_5^-$, of low intensity, is not due to a protonation by H_2O, but by protonation by methanol involving $C_5O_5(CH_3OH)_m^{2-}$ ions originating from the solvent used for electrospray. This

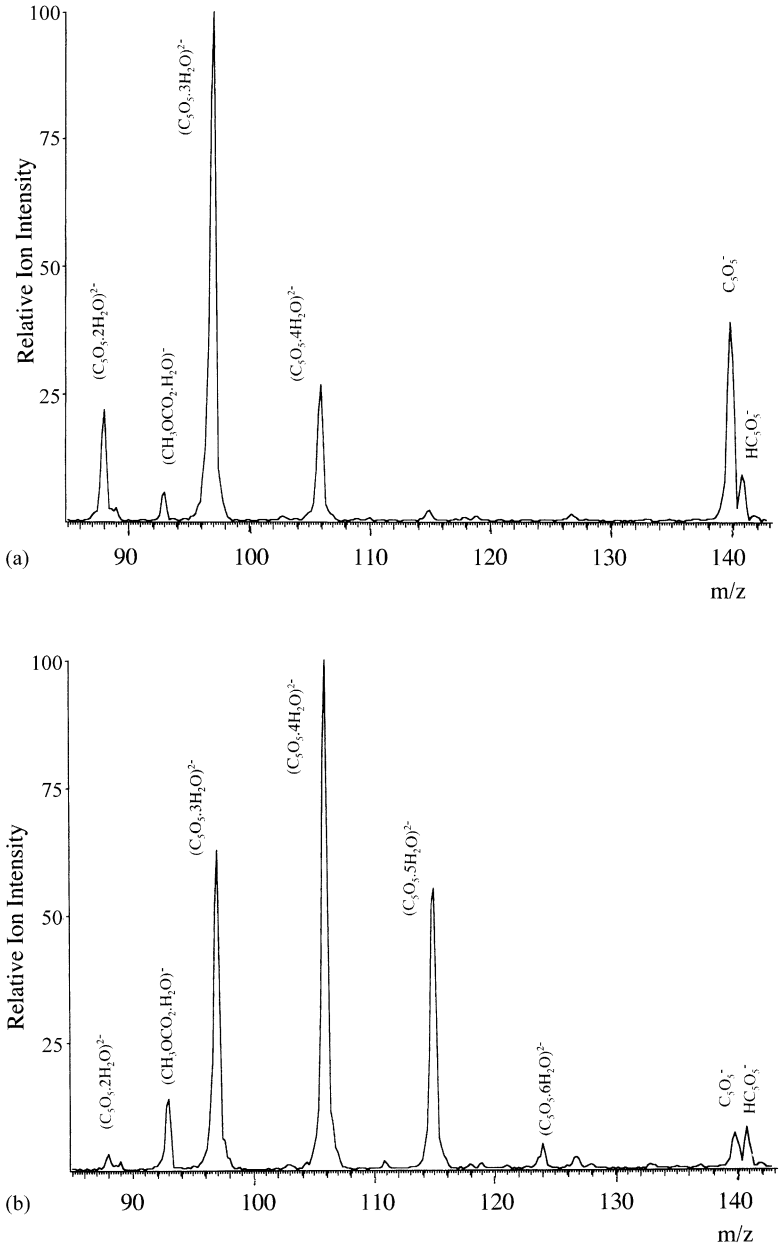

Fig. 2. (a) Ions observed at a higher temperature of 51 °C, relative to Fig. 1. H_2O pressure, 2 mTorr. Not only is the hydrates number *n* lower than in Fig. 1a, but also charge loss has occurred at the higher temperature. The $C_5O_5^-$ ion is due to thermal electron detachment probably mostly from $C_5O_5(H_2O)_2^{2-}$. The smaller $HC_5O_5^-$ peak is attributed to charge loss by proton transfer from methanol molecules, see text. (b) Ions observed at 51 °C and higher H_2O pressure of 8.2 mTorr. Not only is the hydration shifted to higher *n* values of $C_5O_5(H_2O)_n^{2-}$, but also charge loss has been suppressed due to the stabilization by hydration. Note much lower $C_5O_5^-$ and $HC_5O_5^-$ relative to (a).

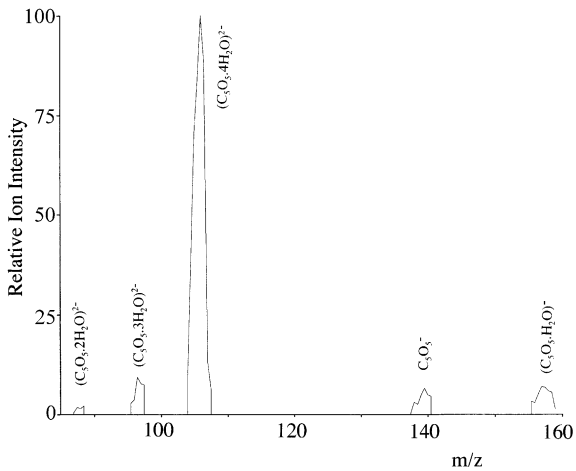

Fig. 3. Results from CID of $C_5O_5(H_2O)_4^{2-}$ ion. The lower hydrates down to $C_5O_5(H_2O)_2^{2-}$ and charge reduced $C_5O_5^-$ and $C_5O_5(H_2O)^-$, were the only CID products observed. Absence of $C_5O_5(H_2O)^{2-}$ product indicates that this monohydrate is unstable and detaches one electron.

conclusion also agrees with the lack of $HC_5O_5^-$ product from the CID of the $C_5O_5(H_2O)_4^{2-}$ ion (Fig. 3).

3.2. Comparison of experimental results for charge reduction with theoretical predictions. Electron detachment. Existence of energy barrier for electron detachment from dianions

The experimental evidence for the occurrence of the electron detachment reaction (Eq. (2)) can be compared with the predictions of the DFT calculations. The structures obtained are summarized in Fig. 6. The energies are given in Table 1. Reaction (1) (Table 1) shows that electron detachment from $C_5O_5^-$ is endothermic by 98.5 kcal/mol, i.e., the electron affinity $EA(C_5O_5) = 98.5$ kcal/mol. This is a very high value, higher than the $EA(F) = 78.4$ kcal/mol, a case where

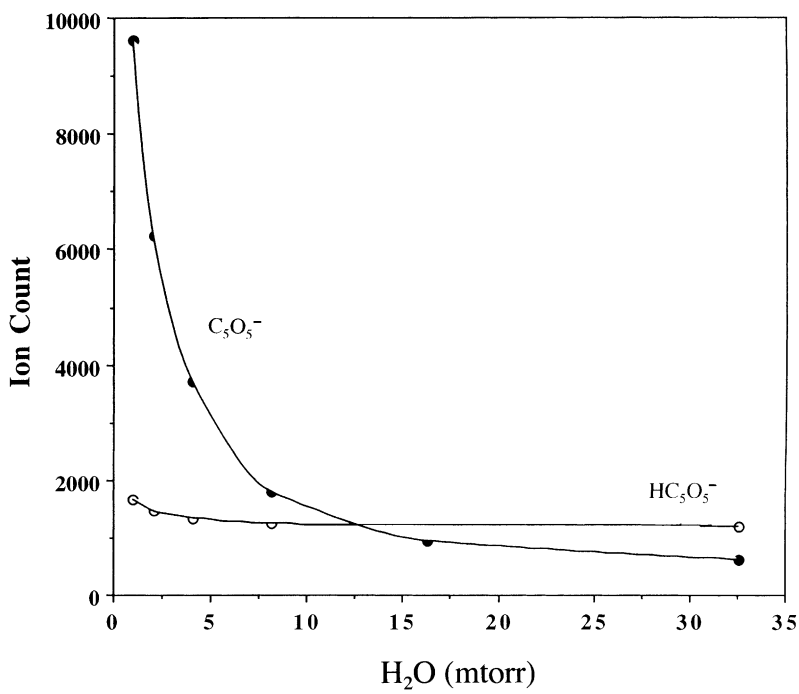

Fig. 4. Plot of observed singly charged products from mass spectra, such as shown in Fig. 2a and b, at 51 °C and several pressures of H_2O. Results show that $C_5O_5^-$ decreases with H_2O pressure, as expected, due to increasing stabilization in the higher n, $C_5O_5(H_2O)_n^{2-}$, hydrates present at higher pressure. On the other hand, $HC_5O_5^-$ is seen to remain constant with H_2O pressure. This result indicates that $HC_5O_5^-$ is due to reactions occurring outside the reaction chamber.

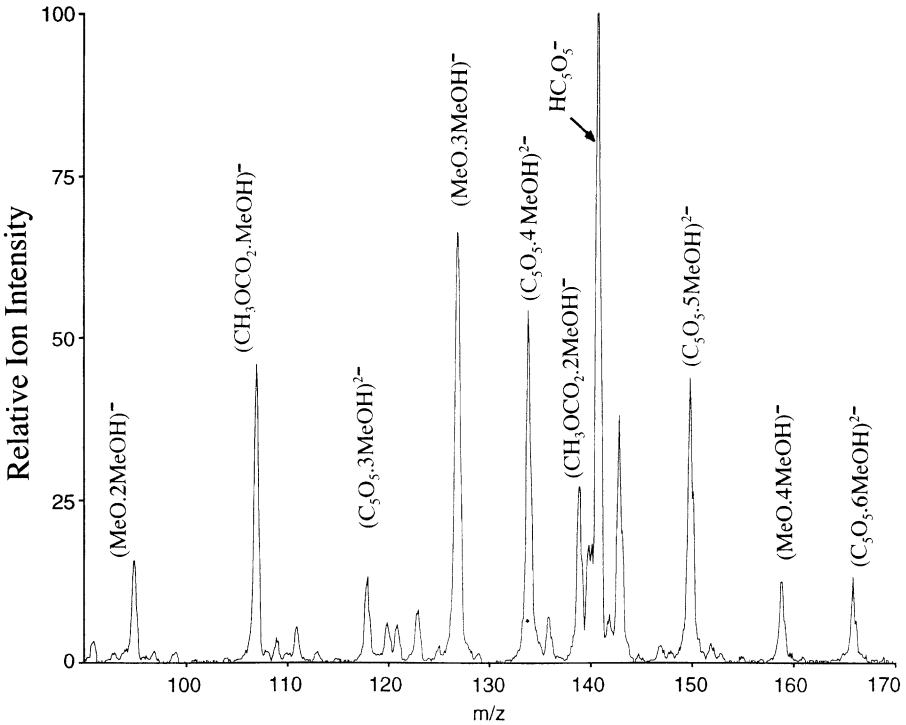

Fig. 5. Ions observed with CH_3OH at 5.5 mTorr in the reaction chamber at 25 °C. The doubly charged solvates, $C_5O_5(CH_3OH)_n^{2-}$, are observed. However, high intensities of singly charged products such as $CH_3O(CH_3OH)_n^-$ and $HC_5O_5^-$, are also observed. Only very small intensities of the methanol solvates of $HC_5O_5^-$ were present. The singly charged ions must be due to the charge separation reaction: $C_5O_5(CH_3OH)_n^{2-} = HC_5O_5^- + CH_3O(CH_3OH)_{n-1}^-$. This reaction probably occurs from the lowest n $C_5O_5(CH_3OH)_n^{2-}$ species. The amount of solvation by CH_3OH observed in the spectrum is not indicative of the solvation in the original products of the charge separation reaction, but is due to further solvation reactions of these products with methanol.

the most electronegative atom and a half filled bonding orbital is involved.

On the other hand, the singly charged $C_5O_5^-$ ion has a negative electron affinity $EA(C_5O_5^-) = -26.0$ kcal/mol (reaction (2), Table 1). Also negative is the $EA(C_5O_5 \cdot H_2O^-) = -13.8$ kcal/mol (reaction (3), Table 1) in agreement with the noted absence of the $C_5O_5^{2-}$ and the $C_5O_5(H_2O)^{2-}$ ion in the experiments (Section 3.1).

The prediction $EA(C_5O_5{\cdot}2H_2O^-) = -2.3$ kcal/mol (reaction (4), Table 1) may appear to disagree with the observation of stable $C_5O_5(H_2O)_2^{2-}$ ions at temperatures as high as 50 °C, see Fig. 2a. However, when doubly charged negative ions are involved, an exothermic electron detachment energy does not necessarily indicate that thermal electron detachment will occur, as is the case for singly charged ions [21]. A considerable energy barrier will be present in the thermal detachment from doubly charged negative ions. This barrier is of Coulombic origin and is most easily perceived by examining the reverse process. The approach of the electron from infinity to the singly charged negative ion is impeded by the Coulombic repulsion between the two charges. Thus, on detachment of the electron from the doubly charged ion a considerable kinetic energy will be released to the leaving electron due to the Coulombic repulsion between it and the remaining one negative charge on the anion. That kinetic energy is not taken into account by the ab initio calculated energies of the separated reactants $C_5O_5(H_2O)_n^{2-}$ and $C_5O_5(H_2O)_n^-$ in Table 1, that are used to obtain the $EA(C_5O_5{\cdot}nH_2O^-)$ values.

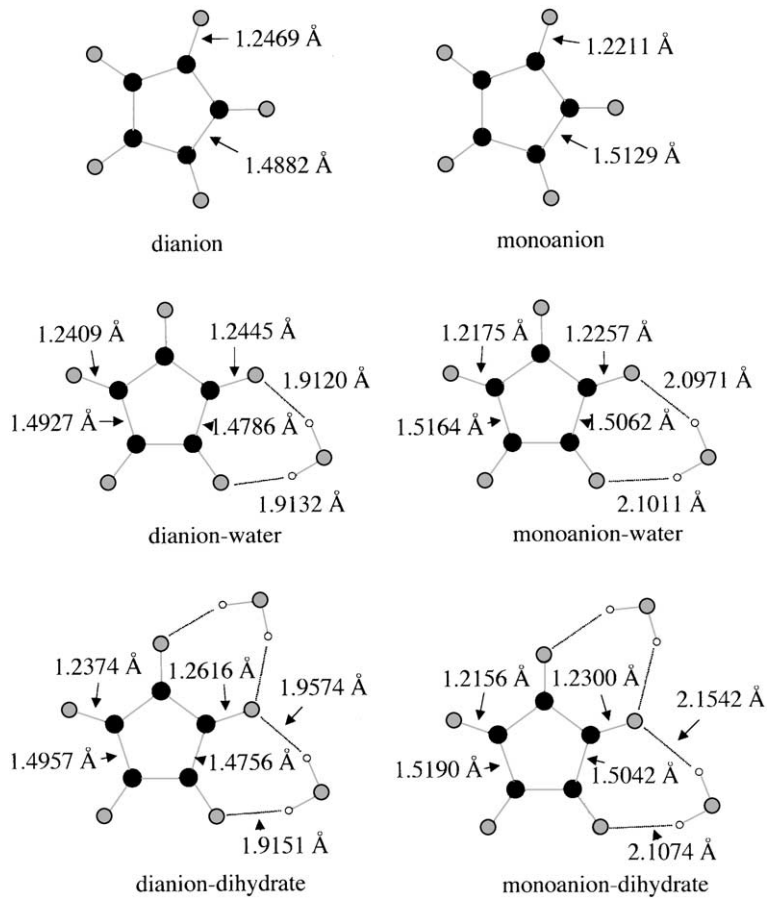

Fig. 6. Structures of $C_5O_5(H_2O)_n^{2-}$ and $C_5O_5(H_2O)_n^{-}$ for $n = 0$, 1, 2 obtained from DFT calculations at the B3LYP/6-311++G(d,p) level.

A schematic, qualitative representation of the barrier for $C_5O_5^{2-}$ is shown in Fig. 7. The solid curve represents the classical Coulomb potential energy that would be approximately valid, once the electron has left the HOMO of $C_5O_5^{2-}$ and is at a distance of several Å from it. The Coulomb energy curve indicates that the barrier will be high, some several tens of kcal/mol at small distances and also quite broad. However, because the energy of the electron in the HOMO is high, corresponding to 26 kcal/mol in the diagram, the electron could be expected to tunnel through the barrier, after an activation energy of less than 10 kcal/mol has been provided by thermal activation. The doubly charged, singly hydrated $C_5O_5(H_2O)^{2-}$ ion was also not observed in the experiments at 50 °C, presumably because it had detached an electron. The energy of the electron in the HOMO in this case is 13.8 kcal/mol (Table 1) and adding an assumed activation energy of some 15 kcal/mol at 50 °C, could be sufficient for the electron to tunnel through the Coulomb barrier that is approximately some 3–4 Å in width at that height.

The above discussion and Fig. 7 provide only a “ballpark view”. Certainly, more quantitative approaches are required. The disintegration of atomic nuclei to two positively charged nuclear particles represents an analogous case in the positive charge domain. This seems to be the first case that was examined theoretically. For an illustration of the barrier (see Fig. 10, Chapters 11 and 12, in Bohm [24]).

Table 1
Theoretical electron detachment and hydration energies of $C_5O_5(H_2O)_n^{m-}$ ($n = 0, 1, 2$), ($m = 1, 2$)

Reaction	ΔE[a] (kcal/mol)
$C_5O_5^-(C_s)$[b] $\rightarrow C_5O_5(D_{5h}) + e^-$	98.5
$C_5O_5^{2-}(D_{5h}) \rightarrow C_5O_5^-(C_s)$[b] $+ e^-$	−26.0
$C_5O_5(H_2O)^{2-} \rightarrow C_5O_5^-(H_2O)^- + e^-$	−13.8
$C_5O_5(H_2O)_2^{2-} \rightarrow C_5O_5^-(H_2O)_2^- + e^-$	−2.3
$C_5O_5(H_2O)^- \rightarrow C_5O_5^- + H_2O$	11.8
$C_5O_5(H_2O)_2^- \rightarrow C_5O_5(H_2O)^- + H_2O$	10.5
$C_5O_5(H_2O)^{2-} \rightarrow C_5O_5^{2-} + H_2O$	24.0[c]
$C_5O_5(H_2O)^{2-} \rightarrow C_5O_5^{2-} + H_2O$	18.0[d]
$C_5O_5(H_2O)_2^{2-} \rightarrow C_5O_5(H_2O)^{2-} + H_2O$	22.0[c]

[a] Energies are computed at the B3LYP/6-311++G(d,p) level of theory and given in kcal/mol.
[b] $C_5O_5^-$ is structurally very close to D_{5h} symmetry but the wave function cannot be expressed within that symmetrical constraint.
[c] H_2O molecule is bonded by two H bonds (see Fig. 6).
[d] H_2O molecule is bonded by one H bond.

Much more recently photodetachment experiments from dianions, where the kinetic energy of the released electron is also determined, have been reported by Wang and co-workers [25,26]. This work includes also estimates of the energy barriers.

3.3. Consecutive hydration energies of $C_5O_5^{2-}$, from equilibrium determinations and theoretical calculations

The ion hydrates, $C_5O_5(H_2O)_n^{2-}$ observed in the mass spectra of Figs. 1 and 2 are in equilibrium. Tests demonstrating the presence of equilibrium ($n-1$,n)

$$C_5O_5(H_2O)_{n-1}^{2-} + H_2O = C_5O_5(H_2O)_n^{2-} \quad (n-1, n) \qquad (4a)$$

$$K_{n-1,n} = \frac{I_n}{(I_{n-1} \cdot pH_2O)} \qquad (4b)$$

$$\Delta G_T^\circ = -RT \ln K_{n-1,n} \qquad (4c)$$

where the ion intensity ratio is assumed to be equal to the concentration ratio of the hydrates [15] and pH_2O is the known partial pressure of H_2O in the reaction chamber, are given in Fig. 8 for $(n-1, n) = (6, 7)$ and (7,8). The linear plots with intercepts at the origin, observed in Fig. 8 obey the equilibrium condition expressed by Eq. (4b) and the slope of the plots corresponds to $K_{n-1,n}$. Determinations of the equilibrium constants, $K_{n-1,n}$, from such plots at different temperatures, lead via van't Hoff plots to the enthalpies

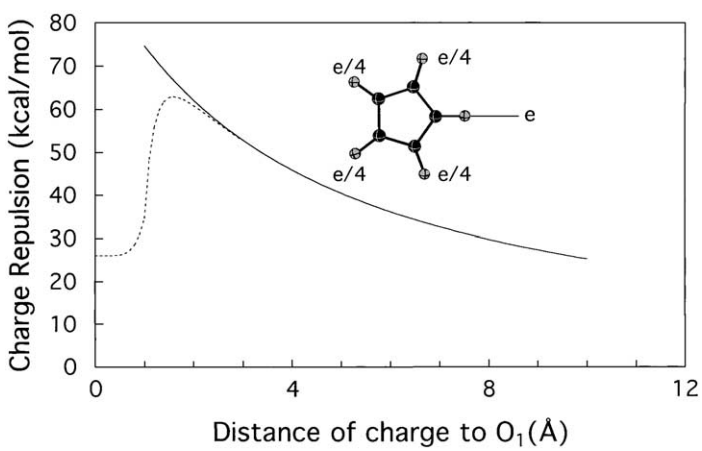

Fig. 7. Qualitative schematic representation of energy barrier for the detachment of an electron from $C_5O_5^{2-}$. The Coulomb barrier for the reverse reaction, the electron attachment, was evaluated with the Coulomb equation and a charge distribution as shown in the inset. The distance between the electron and the O atom, used as the horizontal coordinate is also shown in the inset. As the electron approaches closely the singly occupied orbital, the energy decreases (dashed curve). Energy of 26 kcal/mol shown at very small distances corresponds to electron being in the orbital, see theoretical result in Table 1. Combined curves indicate that tunneling of the electron through the barrier could be expected at moderate temperatures.

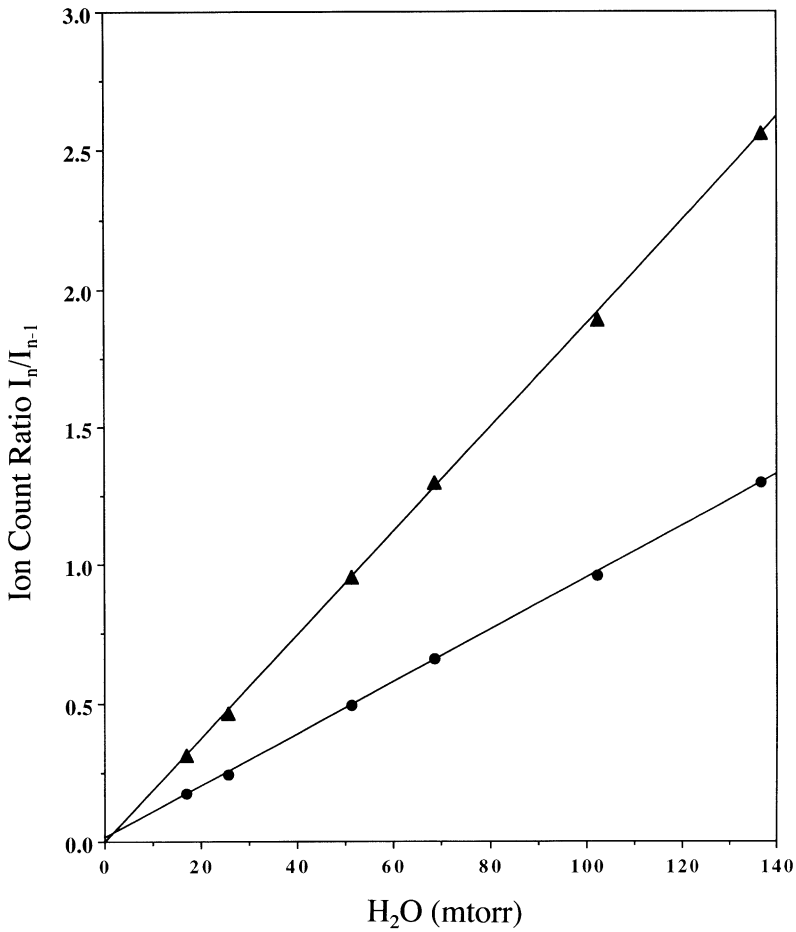

Fig. 8. Determination of hydration equilibrium constants for $(n-1, n) = (6, 7)$ and (7,8). The linear plots with intercepts at the origin obey the equilibrium condition expressed by Eq. (4b) and the slope of the plots corresponds to $K_{n-1,n}$.

$\Delta H^\circ_{n-1,n}$ and $\Delta S^\circ_{n-1,n}$. These are obtained from the slope and the intercept of the linear van't Hoff plots. Shown in Fig. 9 are two such plots that are for the (4,5) and the (5,6) equilibrium. Unfortunately, the temperature range that could be covered was very restricted, because electron detachment, see Eq. (2) and associated discussion, set an upper limit of the temperature at ~50 °C. ΔH° and ΔS° values could be obtained only for (3,4) and higher $(n-1,n)$ values. The data obtained are summarized in Table 2. Energy values for (0,1) and (1,2) that could not be measured experimentally were obtained from DFT calculations and are given in Table 1.

Table 2
Sequential hydration energies[a] of croconate anion $C_5O_5^{2-}$

$(n,n-1)$[b]	$\Delta G^\circ_{n,n-1}$ (298 K)	$\Delta H^\circ_{n,n-1}$	$\Delta S^\circ_{n,n-1}$
(3,2)	10.0	–	–
(4,3)	8.5	17.2	30
(5,4)	7.1	14.0	23.2
(6,5)	5.6	12.1	21.8
(7,6)	5.1	12.6	25.2
(8,7)	4.6	10.6	20.1
(9,8)	3.9	–	–

[a] Energy changes for $\Delta H^\circ_{n,n-1}$ and $\Delta G^\circ_{n,n-1}$ in kcal/mol, $\Delta S^\circ_{n,n-1}$ in cal/mol K. Standard states, 1 atm.

[b] The $(n,n-1)$, rather than the $(n-1,n)$ values are quoted because the $(n,n-1)$ values are positive for ΔG, ΔH and ΔS and thus facilitate the discussion.

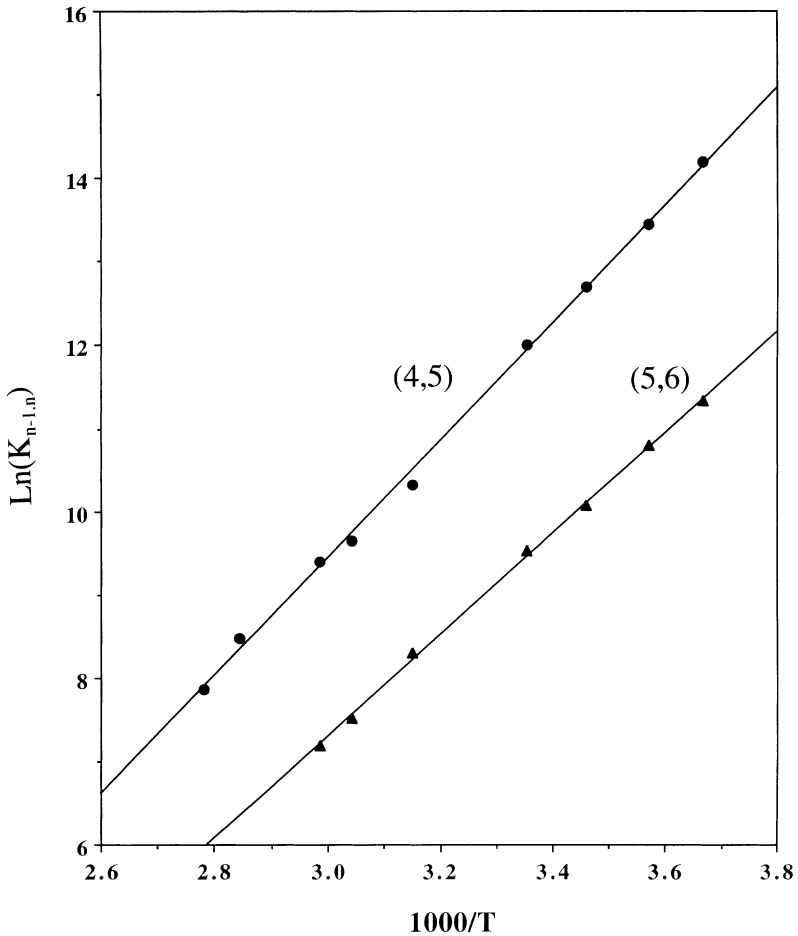

Fig. 9. van't Hoff plots of the equilibrium constants for the (4,5) and (5,6) hydration reactions. Intercepts with vertical axis lead to $\Delta S^{\circ}_{n-1,n}$ while the slopes lead to $\Delta H^{\circ}_{n-1,n}$.

A plot of the most abundant data set, the $\Delta G^{\circ}_{n-1,n}$ at 298 K, vs. n, is shown in Fig. 10. In Table 2 and Fig. 10, we use the energies for the reverse of reaction (Eq. (2)), i.e., the $(n,n-1)$ reaction because the values of $\Delta G^{\circ}_{n,n-1}$, $\Delta H^{\circ}_{n,n-1}$ and $\Delta S^{\circ}_{n,n-1}$ are positive and this facilitates the discussion of the results. For comparison, also included in the figure are $\Delta G^{\circ}_{n,n-1}$ at 298 K values for the hydration of SO_4^{2-} and the dicarboxylate $CO_2(CH_2)_4CO_2^{2-}$ that were obtained in previous determinations [27].

The previous work [27] included hydration determinations of several other oxoacid dianions (see Table 3 and Fig. 7 in [27]). On the basis of those data it was concluded that the magnitude of the energies, $\Delta G^{\circ}_{n,n-1}$ at 298 K depend mainly on two factors. The net negative charge on the oxygen atoms that are involved as H bond acceptors and the proximity of these atoms to each other [27]. The proximity rule is easily checked with the $CO_2(CH_2)_pCO_2^{2-}$ dianions, where it was found that the $\Delta G^{\circ}_{n,n-1}$ value decreases with increase of p. The ion SO_4^{2-} has by far the highest $\Delta G^{\circ}_{n,n-1}$ value of all oxoacids that were determined [27] and that result follows the proximity rule. However, one can expect also that the net negative charge per O atom is higher in SO_4^{2-} than is the case for the dicarboxylic acids because of the higher electron

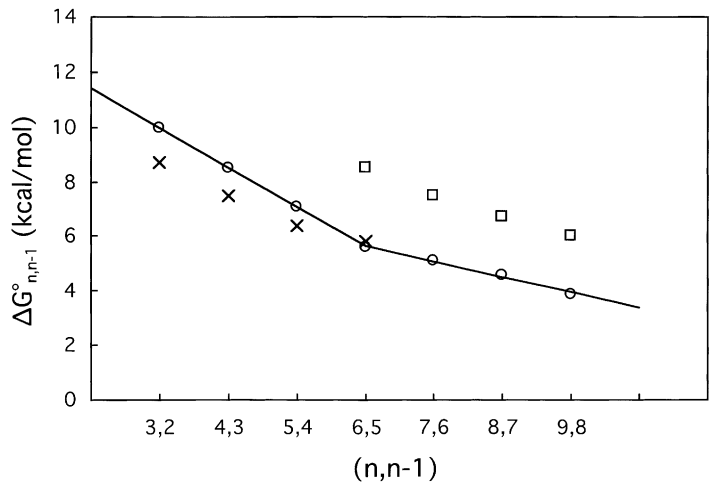

Fig. 10. Plot of $\Delta G^{\circ}_{n,n-1}$ at 298 K, vs. n for reaction: $C_5O_5(H_2O)_n^{2-} = C_5O_5(H_2O)_{n-1}^{2-} + H_2O$ (○). Also shown for comparison are results from earlier determinations of $\Delta G^{\circ}_{n,n-1}$ for the hydration of $CO_2(CH_2)_4CO_2^{2-}$ (×) [27] and SO_4^{2-} (□) [27].

donor ability of the S atom. The charge proximity rule is also expected on the basis of the total hydration energies of doubly charged ions. These are known to increase in exothermicity as the ion radius decreases. This increase can be viewed as a consequence of the charge proximity rule.

The $\Delta G^{\circ}_{n,n-1}$ data in Fig. 10 show a decrease in the order: $SO_4^{2-} \gg C_5O_5^{2-} > CO_2(CH_2)_4CO_2^{2-}$. The observation: $C_5O_5^{2-} > CO_2(CH_2)_4CO_2^{2-}$, can be expected from the proximity rule. However, the double charge in $C_5O_5^{2-}$ is spread over five O atoms rather than four as is the case for $CO_2(CH_2)_4CO_2^{2-}$ and this consideration could lead one to assume a lower charge on the O atoms of $C_5O_5^{2-}$. But regardless of possible small differences between the charge on individual oxygen atoms of $C_5O_5^{2-}$ and $CO_2(CH_2)_4CO_2^{2-}$, the remaining charges are relatively close by in $C_5O_5^{2-}$ complexes, while for the $CO_2(CH_2)_4CO_2^{2-}$ complex one unit of charge is relatively far away with respect to the ligand molecule.

The $\Delta G^{\circ}_{n,n-1}$ values depend also on $\Delta S^{\circ}_{n,n-1}$. It was found in previous work [15] on the diprotonated diamines $(NH_3(CH_2)NH_3)^{2+}$, where the hydration equilibrium could be determined over a wide $(n,n-1)$ and a wide temperature range (so that reliable $\Delta S^{\circ}_{n,n-1}$ could be obtained), that significant contributions to differences in successive $\Delta S^{\circ}_{n,n-1}$ values at low n were due to rotational symmetry number changes. A similar situation is expected also for $C_5O_5^{2-}$, however, the changes will occur mainly in the lowest $n,n-1$ cases. Therefore, the $\Delta G^{\circ}_{n,n-1}$ values present in Fig. 10, that start at (3,2) are expected to follow fairly closely the $\Delta H^{\circ}_{n,n-1}$ changes with n and reflect H bonding differences as assumed in the discussion above.

A transition from an inner to an outer hydration "shell" is expected for the $C_5O_5^{2-}$ hydrates after $C_5O_5(H_2O)_5^{2-}$. The data in Fig. 10 lead to two approximately straight lines one including $\Delta G^{\circ}_{5,4}$ and the other starting with $\Delta G^{\circ}_{6,5}$ that exhibits a slower "fall off" of the values. This indicates weaker $\Delta H^{\circ}_{n,n-1}$ interactions for $n > 5$ as observed in Table 2. Such weaker interactions could be due to a doubling of the water molecules per O atom on the $C_5O_5^{2-}$ such that each H_2O molecule forms a single H bond to the oxygens.

Even though experimental ΔG° values for the 1,0 and 2,1 hydration reactions are not available, those values can be estimated on the basis of the computational electronic binding energies given in Table 1. The theoretical structures for the hydrates (see Fig. 6) clearly show that each water ligand is bound to two

oxygen atoms on the croconate anion. These tight structures lead to loss of rotational freedom relative to the singly H bonded case and this should lead to a higher $\Delta S^{\circ}_{n,n-1}$ term. Using the relatively common $\Delta S^{\circ}_{n,n-1}$ term of 28–30 cal/mol K for a tightly bound ligand to obtain the $T\,\Delta S^{\circ}_{n,n-1}$ term, one obtains estimated $\Delta G^{\circ}_{n,n-1}$ values that fall right in line with the experimental values, as shown in Fig. 10.

Notable for the monohydrate dianion are the increased bond distances of the C–O bonds that interact with the water molecule relative to the C–O bonds that don't interact and the shortening of the C–C bond between the interacting C–O groups. These differences indicate that the H-bonding is strengthened by an increase of charge density on the interacting O atoms and a polarization of the π electron system of the $C_5O_5^{2-}$ leading to a higher C–C electron density on interacting side. This electron density leads to a strengthening of the H-bonds and also the C–C double bond. For the monohydrate monoanion a similar observation is made.

The tightly bound structure is not too surprising for the dianion where the interaction of the water with two oxygens rather than one would gain energetically more than it would lose due to the less than optimal dipole arrangement with respect to the closest oxygen. For the monoanion the energetic gain is less, however, for both there is an additional gain because the dipole alignment although not optimal for the closest oxygen atom is optimal for the total charge on croconate. Some calculations were carried out with alternative arrangement of water on the monoanion but have ultimately converged back to the double interaction that is shown in Fig. 6.

For the dihydrates of both, the monoanion and dianion, a minimum was found that places water on adjacent O–C–C–O interaction sites. This arrangement which places the two water molecules on the same side appears counterintuitive. But, it is favored because it allows for a larger polarization of the croconate anions that stabilizes the bonding. That the polarization has increased can be seen by the C–O bond length of 1.2616 Å for the dianion compared to 1.2445 and 1.2300 Å for the monoanion compared to 1.2257 Å. However, while the polarization has increased, there is also now some repulsion from the partially opposing dipoles of the two water ligands. Evidence for this comes from the difference in the hydrogen bond lengths of the near and far interaction with respect to the two ligands, 1.9151 Å vs. 1.9574 Å (see Fig. 6).

3.4. Formation of complexes $C_5O_5(B)_m(H_2O)_n^{2-}$ with compounds B, such as nitrobenzene, that have positive electron affinities

As discussed in Sections 3.1–3.3, charge reduction for multiply charged negative ions can occur via two different mechanisms: proton transfer from a ligand like a methanol or water molecule or electron loss by electron detachment. Electron detachment can be promoted not only by thermal/CID activation and photons (photodetachment) but also by electron transfer to a molecule with positive electron affinity EA. (For determinations of EA's of molecules with positive EA, by electron transfer equilibrium involving singly charged negative ions, see [28].) The charge loss by electron transfer involving multiply charged anions should be distinctly different from charge loss by proton transfer because the transition is not a gradual shift of the proton, with a transition state, but corresponds to electron tunneling through the Coulomb barrier, see Section 3.2 and Fig. 7. We thought that it would be interesting to explore experimentally electron transfer from the hydrates $C_5O_5(H_2O)_n^{2-}$ to molecules with positive electron affinities.

One of the first molecules used was nitrobenzene (NB) whose EA(NB) = 23 kcal/mol [28]. Instead of electron transfer, adduct formation involving the hydrates $C_5O_5(H_2O)_n^{2-}$ and NB was observed as illustrated by the mass spectrum (Fig. 11). The hydrates, $C_5O_5(H_2O)_n^{2-}$ with a maximum at $n = 4$, that dominated the spectrum in the absence of NB (9 mTorr H_2O pressure and 55 °C temperature, see Fig. 2b) were reduced to less than one-tenth of their intensity in the simultaneous presence of only 0.12 mTorr of NB in the reaction chamber. The resulting $C_5O_5(H_2O)_n(NB)_m^{2-}$ are shown in the mass spectrum (Fig. 11), that includes only the higher intensity

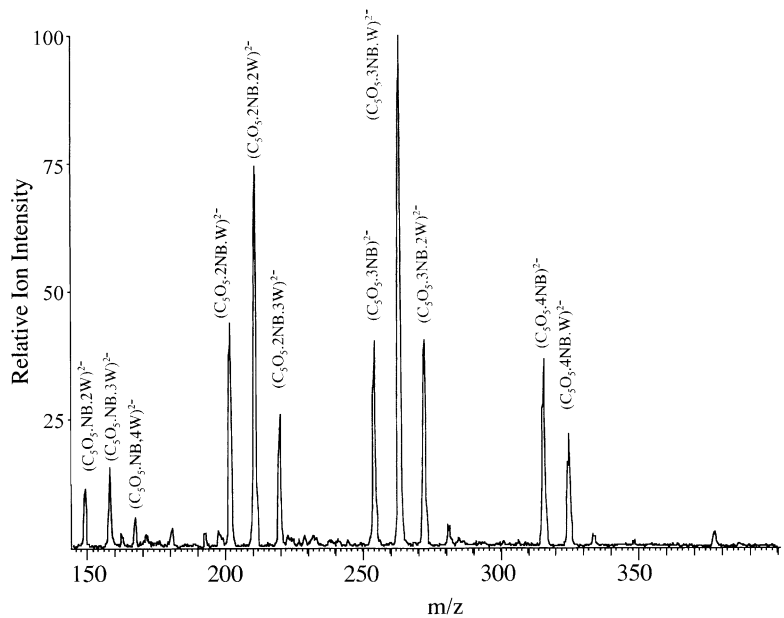

Fig. 11. Ions observed when 0.12 mTorr of nitrobenzene (NB) was added to the reagent gas mixture containing 8.7 mTorr water and 8.6 Torr of the bath gas N_2 at 55 °C. Mixed cluster ions $C_5O_5(H_2O)_n(NB)_m{}^{2-}$ dominate the mass spectrum. High intensities are observed for species where $m + n = 5$.

ions of the group $C_5O_5(H_2O)_n(NB)_m{}^{2-}$. Maximum intensity is observed for the $C_5O_5(H_2O)_1(NB)_3{}^{2-}$ ion. The maximum intensity for a hydrate group with a given $(NB)_m$ occurs at $m + n = 4$, see Fig. 11. Furthermore, an abrupt decrease of intensity for each m group occurs when $m + n$ changes from $m + n = 5$ to $m + n = 6$, see Fig. 11. These results strongly suggest that the NB molecules are replacing the H_2O molecules by bonding to the five oxygen atoms of the $C_5O_5{}^{2-}$ in the plane of the C_5O_5 molecule. The ability of NB to replace H_2O when the partial pressure ratio is: $H_2O/NB = 75$, indicates that the interaction with NB leads to a free energy that is in the average some 2.8 kcal/mol more exoergic than that with H_2O. The abrupt decrease of intensity above $n + m = 5$ indicates that in the presence of NB the stability of the solvated cluster decreases sharply above, $n + m = 5$, i.e., when the inner "shell" is completed.

The nature of the bonding of NB to the partially negative O atoms of $C_5O_5{}^{2-}$ indicated by the above results, could be largely of electrostatic nature and similar to the H bonding of the H_2O. Experiments where benzene vapor was added instead of NB showed no complex formation, indicating that the presence of the nitro group is essential. Similarly, no complex formation was observed in experiments with cyano-perfluorobenzene, a compound that has a positive electron affinity but no H atoms.

Therefore, for the NB containing complexes a structure involving the phenyl H atom in position 4 to the nitro group that "hydrogen bonds" to an oxygen on the $C_5O_5{}^{2-}$ is indicated by the results in Fig. 11. The nitro group is known to have a strong electron withdrawing field effect [29] and the phenyl group is quite polarizable. Preliminary results based on DFT calculations of the monosolvate $NB{\cdot}C_5O_5{}^{2-}$ also support such a structure. The binding energy predicted by the calculation is 28 kcal/mol, which is higher than the binding energy for a water monosolvate, particularly when the water is bonded by only one H bond. Calculations for the one H bond structure lead to 18 kcal/mol, some 6 kcal/mol lower than the two H bond structure, see Table 1. The stronger bonding to NB predicted by the calculations is in qualitative agreement with the higher

average $\Delta G^{\circ}_{n,n-1} = 2.8$ kcal/mol, for NB relative to H_2O, obtained from the experimental results for the polysolvates. Previous determinations of the bonding of the chloride ion Cl^- to substituted benzenes [30a] and to H_2O [30b] also show a stronger bond free energy by some 2.3 kcal/mol with NB. Furthermore, theoretical calculations [30a] also support the H bonded structure for NB–Cl^-.

Hiraoka and co-workers [31] observed the dimer formation:

$$C_6F_6{}^- + C_6F_6 = (C_6F_6)_2{}^- \quad (5)$$

in a high pressure mass spectrometer. On the basis of STO-3G ab initio calculations, they proposed a structure involving a stacking of the two perfluorobenzenes due to an attractive interaction of the singly occupied SOMO orbital of the $C_6F_6{}^-$ with the LUMO of the C_6F_6. These two orbitals are degenerate in the absence of an electron. The distance between the two stacked rings was 3.88 Å. Structures for where the C_5O_5 and NB are stacked while the H_2O molecules are at the periphery of the C_5O_5 molecule are not expected for the $C_5O_5(H_2O)_n(NB)_m{}^{2-}$ complexes, on the basis of the experimental evidence based on the observation that the ligand number tends towards $m+n=5$. They are also not likely because the symmetry of the C_6 and C_5O_5 rings is different.

The $C_5O_5{}^{2-}$ solvates in Fig. 11 are connected by rapid equilibrium reactions. Therefore, the participation of any the solvates in an electron transfer reaction to NB, followed by formation of free NB^- and the solvated mono-anion $C_5O_5{}^-$, will lead to rapid disappearance of all of the $C_5O_5(H_2O)_n(NB)_m{}^{2-}$ solvates. Clearly such a reaction is not occurring under the conditions used for the Fig. 11 experiments. This means that the lowest solvate $C_5O_5(H_2O)_2(NB)_1{}^{2-}$ that has the weakest stabilization by solvation also does not engage in electron transfer to NB. An energy profile plot for the reactions involving desolvation and electron transfer:

$$C_5O_5(H_2O)_2{}^{2-} + NB \leftarrow (C_5O_5(H_2O)_2(NB))^{2-} \rightarrow C_5O_5(H_2O)_2{}^- + NB^- \quad (6)$$

could be obtained by DFT calculations. Equations for the energies of transition states of the desolvation E_{DS} and electron transfer E_{ET} could then be obtained with electrostatic equations, as was done for the somewhat analogous case of desolvation or proton transfer in doubly charged positive ions [16,19]. Charge separation by proton transfer in positive ions is an area that has received much more attention [16,17,19,32]. The electrostatic equations are particularly useful when predictions for a series of reactions involving the same doubly charged ion and different neutral reactants (ligands) is involved. An important difference in the electron transfer case is the presence of tunneling. Predictions of the tunneling rate would require knowledge not only of the maximum (the "transition state") of the Coulomb barrier but also the actual shape (width) of the barrier.

Clearly, additional experimental work on the complexation of $C_5O_5(H_2O)_2{}^{2-}$ with other ligands would be very useful. Such work is in progress. We have preliminary results that show that electron transfer to 1,3-dinitrobenzene, EA = 36.9 kcal/mol [28], is observed at temperatures above 50 °C.

4. Conclusions

(a) The cyclic oxocarbon dianions, such as $C_5O_5(H_2O)_n{}^{2-}$ or $C_5O_5(CH_3OH)_n{}^{2-}$ can be easily produced in the gas phase by electrospray. They represent interesting examples of moderate size symmetric dianions whose solvation energies in the gas phase can be determined.

(b) The $\Delta G^{\circ}_{n,n-1}$ values for the reactions: $C_5O_5(H_2O)_n{}^{2-} = C_5O_5(H_2O)_{n-1}{}^{2-} + H_2O$, exhibit a change of slope, that signals weaker solvation above $n=5$.

(c) Below $n=2$, the hydrates become unstable and exhibit charge separation by thermal electron detachment. When methanol is used instead of water, charge separation occurs not by electron loss but by proton transfer from the methanol molecules. This difference can be attributed to the higher gas phase acidity of methanol relative to water.

(d) $C_5O_5(H_2O)_2^{2-}$ is observed to be stable towards electron detachment even though theoretical DFT calculations predict that electron detachment is exothermic. This result demonstrates that an energy barrier exists for the detachment that is due to the Coulomb repulsion between the $C_5O_5(H_2O)_2^-$ and the detached electron.

(e) DFT calculated electron detachment energies predict exothermicities of 14 and 26 kcal/mol for $C_5O_5(H_2O)^{2-}$ and $C_5O_5^{2-}$. A qualitative examination of the expected Coulomb barrier indicates that the electrons can readily tunnel through it and lead to electron detachment, in agreement with the experimental observations.

(f) Use of molecules with positive electron affinity such as nitrobenzene (NB) (electron affinity EA = 23 kcal/mol) does not lead to electron transfer from $C_5O_5(H_2O)_n^{2-}$ even when the transfer reaction is highly exothermic, as is the case with $C_5O_5(H_2O)_2^{2-}$ (EA $C_5O_5(H_2O)_2^- = -2.3$ kcal/mol). This observation is also attributed to the presence of a Coulomb energy barrier. Instead of electron transfer, bonding of NB to the dianion is observed. The H atom in position 4 of NB forms an H bond to one of the oxygen atoms of the $C_5O_5^{2-}$. The bond is stronger than the H bonds formed by H_2O molecules. However, electron transfer does occur when molecules with higher electron affinities such as 1,3-dinitrobenzene (EA = 36.9 kcal/mol) are used and the stabilization of the dianion by solvation is weak, such as for $C_5O_5(H_2O)_2^{2-}$.

(g) Theoretical predictions whether electron transfer to a ligand with a given electron affinity would be possible, either on the basis of DFT calculations or approximate electrostatic equations, but these must also include consideration of the probability for electron tunneling.

Acknowledgements

Some of the experiments dealing with electron transfer were performed by Dr. Udo Verkerk. This work was supported by a grant from the Natural Sciences Research Council of Canada.

References

[1] R. West (Ed.), Oxocarbons, Academic Press, New York, 1980.
[2] J. Aihara, Bull. Chem. Soc. Jpn. 60 (1987) 2268.
[3] P. Jayaweera, A.T. Blades, M.G. Ikonomou, P. Kebarle, J. Am. Chem. Soc. 112 (1990) 2452.
[4] A.T. Blades, P. Jayaweera, M.G. Ikonomou, P. Kebarle, J. Chem. Phys. 92 (1990) 5900.
[5] A.T. Blades, P. Jayaweera, M.G. Ikonomou, P. Kebarle, Int. J. Mass Spectrom. Ion Process. 102 (1990) 251.
[6] A.A. Shvartsburg, K.W.M. Siu, J. Am. Chem. Soc. 123 (2001) 10071.
[7] J.B. Fenn, M. Mann, C.K. Meng, S.F. Wong, C.M. Whitehouse, Science 246 (1989) 64.
[8] K.G. Spears, F.C. Fehsenfeld, M. McFarland, E.E. Ferguson, J. Chem. Phys. 56 (1972) 2562.
[9] M. Solà, A. Lledós, M. Duran, J. Bertrán, Theor. Chim. Acta 81 (1992) 303.
[10] M. Peschke, A.T. Blades, P. Kebarle, Int. J. Mass Spectrom. 185 (1999) 685.
[11] M. Beyer, E.R. Williams, V.E. Bondybey, J. Am. Chem. Soc. 121 (1999) 1565.
[12] P. Vitorge, M. Masella, Chem. Phys. Lett. 332 (2000) 367.
[13] V.E. Bondybey, M.K. Beyer, Int. Rev. Phys. Chem. 21 (2002) 277.
[14] K.P. Faherty, C.J. Thompson, F. Aguirre, J. Michne, R.B. Metz, J. Phys. Chem. A 105 (2001) 10054.
[15] A.T. Blades, J.S. Klassen, P. Kebarle, J. Am. Chem. Soc. 118 (1996) 12437.
[16] M. Peschke, A.T. Blades, P. Kebarle, J. Am. Chem. Soc. 124 (2002) 11519.
[17] P.D. Schnier, D.S. Gross, E.R. Williams, J. Am. Chem. Soc. Mass Spectrom. 6 (1995) 1086.
[18] D.S. Gross, P.D. Schnier, S.E. Rodriguez-Cruz, C.K. Fagequist, Proc. Natl. Acad. Sci. U.S.A. 93 (1996) 3143.
[19] S. Gronert, J. Am. Chem. Soc. 118 (1998) 3525.
[20] (a) N. Felitsin, M. Peschke, P. Kebarle, Int. J. Mass Spectrom. 219 (1) (2002) 39;
(b) A.T. Blades, M. Peschke, U. Verkerk, P. Kebarle, J. Phys. Chem. A 106 (2002) 10037;
(c) U.H. Verkerk, M. Peschke, P. Kebarle, J. Mass Spectrom. (2003), in press.
[21] E.P. Grimsrud, S. Chowdhury, P. Kebarle, J. Chem. Phys. 83 (1985) 3983.
[22] (a) A.T. Blades, P. Kebarle, J. Am. Chem. Soc. 116 (1994) 10761;
(b) A.I. Boldyrev, J. Simons, J. Phys. Chem. 98 (1994) 2298.
[23] M.J. Frisch, G.W. Trucks, H.B. Schlegel, P.M.W. Gill, G.B. Johnson, M.A. Robb, J.R. Cheeseman, T. Keith, G.A. Petersson, J.A. Montgomery, K. Raghavachari, M.A. Al-Laham, V.G. Zakrzewski, J.V. Oritz, J.B. Foresman, J. Cioslowski, B.B. Stefanov, A. Nanayakkara, M. Challacombe,

C.Y. Peng, P.Y. Ayala, W. Chen, M.W. Wong, J.L. Andres, E.S. Replogle, R. Gomperts, R.L. Martin, D.J. Fox, J.S. Binlkey, D.J. Defrees, J. Baker, J.P. Stewart, M. Head-Gordon, C. Gonzalez, J.A. Pople, Gaussian94, Revision D.3, Gaussian, Inc., Pittsburgh, PA, 1995.

[24] D. Bohm, Quantum Theory, Dover Publications, New York, 1979, p. 241.

[25] (a) L.S. Wang, C.F. Ding, X.D. Wang, J.D. Nicholas, Phys. Rev. Lett. 81 (1998) 2667;
(b) X.B. Wang, C.F. Ding, L.S. Wang, Phys. Rev. Lett. 81 (1998) 3351.

[26] X.B. Wang, C.F. Ding, L.S. Wang, Chem. Phys. Lett. 307 (1999) 391.

[27] A.T. Blades, J.S. Klassen, P. Kebarle, J. Am. Chem. Soc. 117 (1995) 10563.

[28] P. Kebarle, S. Chowdhury, Chem. Rev. 87 (1987) 513.

[29] R.W. Taft, R.D. Topsom, Prog. Phys. Org. Chem. 16 (1987) 1;
G.J.C. Paul, P. Kebarle, Can. J. Chem. 68 (1990) 2070.

[30] G.J. Paul, P. Kebarle, J. Am. Chem. Soc. 113 (1991) 1148;
(b) M. Arshadi, R. Yamdagni, P. Kebarle, J. Phys. Chem. 74 (1970) 1475.

[31] K. Hiraoka, S. Mizuse, S. Yamabe, J. Phys. Chem. 94 (1990) 3689.

[32] V. Baranov, D. Bohme, Int. J. Mass Spectrom. Ion Process. 165/166 (1997) 249.